


Article

Phase Current Measurement Method of Dual Inverter-Motor Drive System Using a Single DC Link Current Sensor

Seon-Ik Hwang ¹, Seong-Hyeon Cho ², Jun-Hyung Jung ³ and Jang-Mok Kim ^{1,*}¹ Department of Electrical Engineering, Pusan National University, Busan 46241, Korea; hsiatop@pusan.ac.kr² Advanced Electricification Engineering Design Team, Hyundai Motor Company, Hwaseong 18280, Korea; seonghyeon.cho@hyundai.com³ Chair of Power Electronics, Kiel University, 24143 Kiel, Germany; jj@tf.uni-kiel.de

* Correspondence: jmok@pusan.ac.kr; Tel.: +82-51-510-2366

Abstract: In recent years, electric propulsion systems have become widely used and these systems have strict limits in volume and weight. Therefore, it is necessary to reduce the weight of the inverter-motor drive system. In a typical n inverter-motor drive system, at least $2n$ phase current sensors are required. In order to reduce the number of phase current sensors, this paper proposes a method for measuring phase current using n DC link current sensors in a $2n$ inverter-motor drive system. Two phase currents per inverter-motor system are measured during one period of the switching frequency using the pulse width modulation (PWM) shift method. However, since the measured phase current contains an error component in the average current, the error component was compensated for in order to obtain a current similar to the actual phase current by using the slope and dwell time of the phase current. The effectiveness of the proposed method is verified through experiments.



Citation: Hwang, S.-I.; Cho, S.-H.; Jung, J.-H.; Kim, J.-M. Phase Current Measurement Method of Dual Inverter-Motor Drive System Using a Single DC Link Current Sensor.

Energies **2021**, *14*, 5626.
<https://doi.org/10.3390/en14185626>

Academic Editors: Sérgio Cruz,
André Mendes and Chunhua Liu

Received: 22 June 2021

Accepted: 2 September 2021

Published: 7 September 2021

Publisher's Note: MDPI stays neutral with regard to jurisdictional claims in published maps and institutional affiliations.



Copyright: © 2021 by the authors. Licensee MDPI, Basel, Switzerland. This article is an open access article distributed under the terms and conditions of the Creative Commons Attribution (CC BY) license (<https://creativecommons.org/licenses/by/4.0/>).

Keywords: dual inverter-motor drive; single DC link current; current reconstruction; PWM shift; SVPWM

1. Introduction

Recently, conventional fuel-powered transportation has been facing major regulations due to environmental problems. For this reason, the transport industry is currently undergoing a transition toward electric-based transportation, such as electric vehicles, ship propulsion, and aircraft systems. In an electric propulsion system, it is necessary to reduce the weight and volume, noise, and vibration while achieving high efficiency. Using several motors in the propulsion system increases the efficiency of the system [1–11].

However, for vector control of motors, three-phase current information is required. In general, a minimum of two current sensors are required in order to obtain a three-phase current, and an additional DC link current sensor is required to protect against overcurrent. Studies have been conducted using a single DC link current sensor to measure the phase currents. When this method is applied, the size and cost of the system can be reduced. However, this method is unable to measure the phase current in all regions and also causes a distortion in the measured phase currents. The phase current is measured when the active voltage vector is applied. However, if the duration of the active voltage vector is shorter than the measurement time of the current, the phase current cannot be measured. In the unmeasurable area, the phase current can be reconstructed by using the pulse width modulation (PWM) shift method, the new voltage modulation method, and the current estimation method. The PWM shift method is a method to secure the dwell time of the active voltage vector by moving the PWM switching pattern left and right within one switching period [12–15]. The new voltage modulation method is to use a different kind of PWM method other than the space vector pulse width modulation (SVPWM) [16–18]. The current estimation method is a method of restoring the current through the current estimation equation using the last current obtained in the measurable area [13,19–21].

The control of a single motor-inverter system using a single DC link current sensor have been studied a lot [12–21]. However, recently the use of multiple motor-inverter systems in one propulsion system is becoming common to improve the efficiency of the overall system. To control two inverter-motor systems, a method of measuring all phase currents using only single DC link current sensor was studied in [6]. However, in the conventional method, each voltage vector is asymmetrically applied to measure the phase current. Therefore, the conventional method increases the phase current ripple compared to the (SVPWM) method, and the noise of the inverter-motor system increases by the increased phase current ripple [6,7].

Therefore, this paper proposes a method to measure the phase current using a single DC link current sensor in a dual inverter-motor system with symmetrical voltage vectors. A new PWM shift method is applied to obtain the phase current from a single DC link current sensor. The two-phase currents of each motor are measured by sequentially sampling a DC link current four times during one switching frequency cycle. Since the measured phase current contains an error component, the average current of the two phases are estimated by compensating for the error component of the phase current. The effectiveness of the proposed method is verified through experiments.

2. Phase Current Measurement Method Using a Single DC Link Current Sensor

2.1. One Inverter-Motor System

The one-shunt inverter is a system that measures the three-phase current of a motor using one DC link current sensor (as shown in Figure 1). A specific phase current flows through the DC link current sensor according to the switching state of the inverter, and can be expressed as follows in Equation (1) [12–21]:

$$I_{DC} = S_a i_a + S_b i_b + S_c i_c \quad (1)$$

where S_x ($x = a, b, c$) is the switching state of phase x . When the upper switch is turned on, S_x is 1, and when the lower switch is turned on, S_x is 0. The switching states and the phase current that can be measured from the DC link sensor during each switching state are shown in Table 1. A specific phase current can be obtained in a section where the active voltage vector is applied, and phase current cannot be obtained in a section where the zero voltage vector is applied.

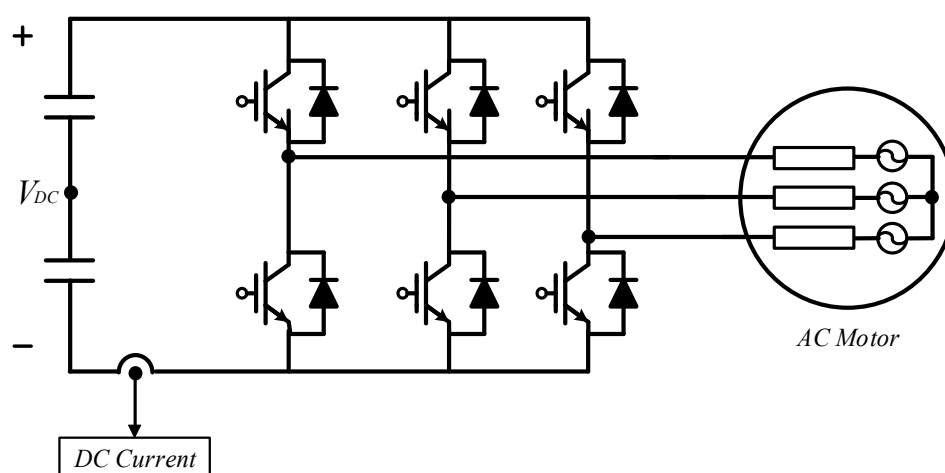


Figure 1. Inverter-motor control system with a single DC link current sensor for measuring phase current.

Table 1. Measurable phase current according to voltage vector using a DC link current sensor.

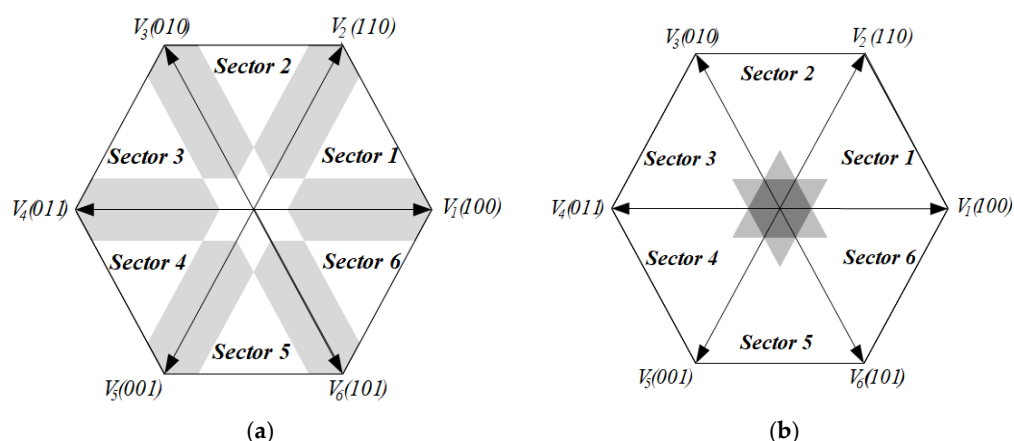
Switching State	Active Voltage Vector					Zero Voltage Vector	
	(100)	(110)	(010)	(011)	(001)	(101)	(000) (111)
i_{DC}	i_a	$-i_c$	i_b	$-i_a$	i_c	$-i_b$	-

However, if the dwell time of the active voltage vector is less than the minimum time (T_{min}) required for current sampling, the phase current cannot be obtained from the single DC link current sensor even when the active voltage vector is applied. The T_{min} can be defined as follows in Equation (2) [6,13–15]:

$$T_{min} = T_{dead} + T_{settling} + T_{ad} \quad (2)$$

where T_{dead} is the dead time used to prevent a short circuit, $T_{settling}$ is the time for the stabilization of the current, and T_{ad} is the conversion delay of the AD converter.

To sample the current, the minimum time given in Equation (2) is required. However, there are regions in the space vector where the dwell time is shorter than the minimum time, as shown in Figure 2. Figure 2a shows the bar regions, which are areas where only one phase current can be sampled from the DC link sensor. Figure 2b is a star region, which is an area where no phase current can be sampled.

**Figure 2.** Classification of the unmeasurable region in the space vector: (a) bar region, (b) star region. (adapted from [13]).

2.2. Dual Inverter-Motor Drive System

Figure 3 shows the dual inverter-motor drive system. The phase currents of this system are measurable using a single DC link current sensor. The DC link current flows in the phase currents of the dual motors according to the switching state of the dual motors, and the relation between the switching sequence and the DC link current can be represented as follows in Equation (3) [6]:

$$I_{DC,T} = I_{DC1} + I_{DC2} = S_{a1}i_{a1} + S_{b1}i_{b1} + S_{c1}i_{c1} + S_{a2}i_{a2} + S_{b2}i_{b2} + S_{c2}i_{c2} \quad (3)$$

where S_{x1} ($x1 = a1, b1, c1$) is switching state of phase x in motor1, and S_{x2} ($x2 = a2, b2, c2$) represents switching functions of phase x in motor2. When the upper switch is turned on, S_x is 1, and when the lower switch is turned on, S_x is 0.

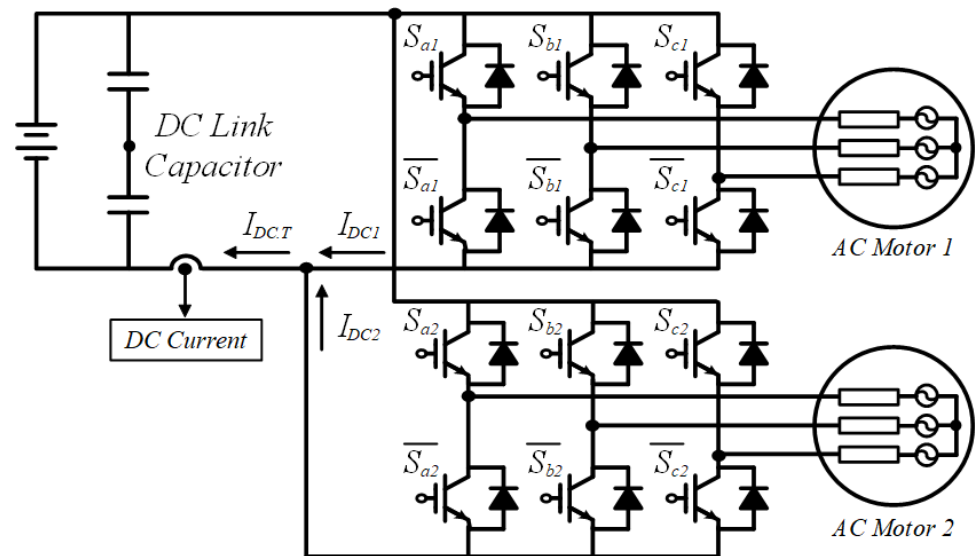


Figure 3. Dual inverter-motor control systems with one current sensor for measuring phase current.

As shown in Equation (3), when the active voltage vector of the dual motors is applied at the same time, the DC link current is the sum of the DC link currents of the dual motors. Therefore, when the active voltage vectors of both motors are applied at the same time, the phase current of each motor cannot be measured from the DC link current at the same time. Therefore, as shown in Equations (4) and (5), if one motor drive system applied the active voltage vector while the other motor drive system is using the zero voltage vector, the phase current of the motor that applied the active voltage vector can be measured from the single DC link sensor.

$$S_{a1}i_{a1} + S_{b1}i_{b1} + S_{c1}i_{c1} \neq 0, S_{a2}i_{a2} + S_{b2}i_{b2} + S_{c2}i_{c2} = 0 \quad (4)$$

$$S_{a1}i_{a1} + S_{b1}i_{b1} + S_{c1}i_{c1} = 0, S_{a2}i_{a2} + S_{b2}i_{b2} + S_{c2}i_{c2} \neq 0 \quad (5)$$

The authors in [6] proposed a PWM shift method shown in Figure 4 in order to secure the point in time at which the phase current of each motor can be measured from the DC link current. After the switching cycle starts, the switching S_{a1} for the maximum of the reference pole voltage in inverter 1 is applied immediately, the switching S_{b1} for the intermediate of the reference pole voltage is applied at time T_{min} , and the switching S_{c1} for the minimum of the reference pole voltage is applied at time $2T_{min}$. Inverter 2 applies switching for the maximum, medium, and minimum reference pole voltages at time $2T_{min}$, $3T_{min}$, and $4T_{min}$, respectively.

By applying this PWM shift method and sampling the DC link current four times at the intervals of T_{min} after switching starts, information on the two-phase current in each motor can be sequentially obtained. In the example of Figure 4, i_{a1} , $-i_{c1}$, i_{b2} , and $-i_{c2}$ can be obtained sequentially from the start of switching.

However, this method applies an active voltage vector asymmetrically to measure the phase current. Therefore, the phase current ripple increases during one switching period, and the noise and vibration of the inverter-motor system increase due to the application of an asymmetric voltage [6,7].

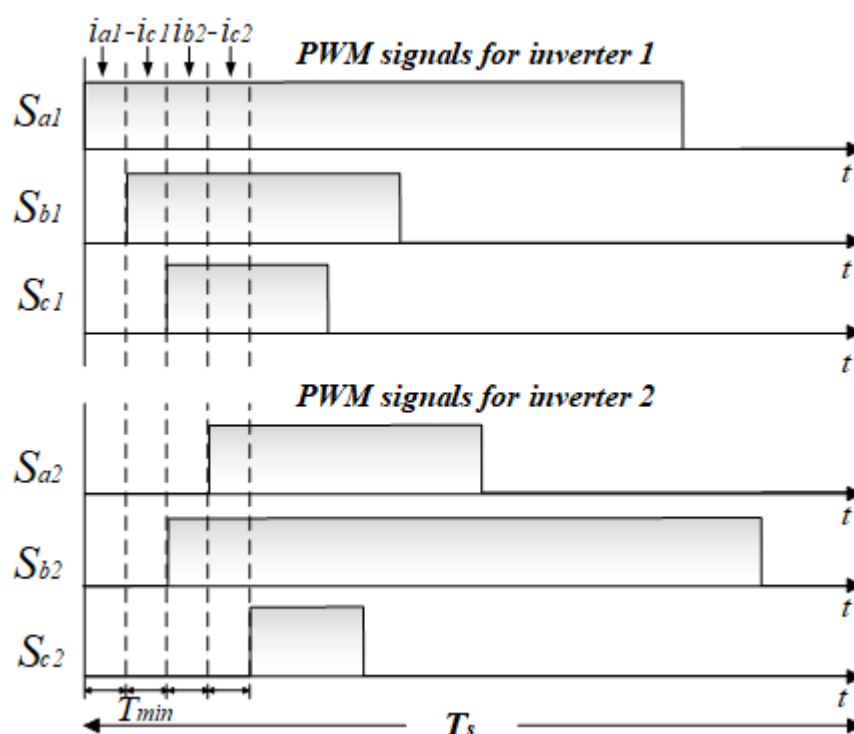


Figure 4. Conventional PWM shift method [6] for measuring the phase current of dual inverters.

3. Proposed PWM Shift Method for Phase Current Measurement in a Dual Inverter-Motor Drive System

3.1. Securing Measuring Time by Offset Voltage

In order to measure the phase current in inverter 1 from DC link current sensor, a simultaneous active voltage vector and zero voltage vector should be applied to inverter 1 and inverter 2, respectively. Therefore, a method of symmetrically shifting the PWM signal of the dual motors is needed in order to secure the point of time for measuring the phase current of the motor. As shown in Figures 5 and 6, offset voltages of different magnitude are applied at the reference three-phase voltage in each motor to secure the timing of the phase current measurement.

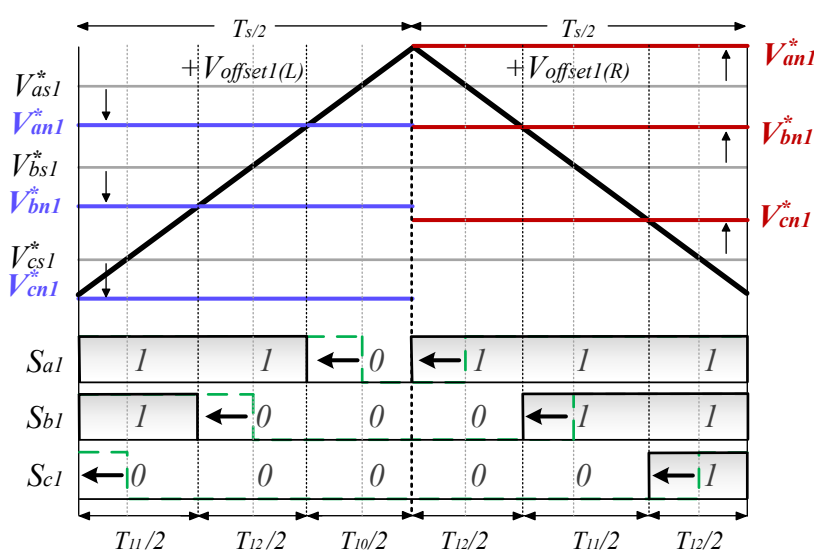


Figure 5. Switching state of inverter 1 with the proposed method.

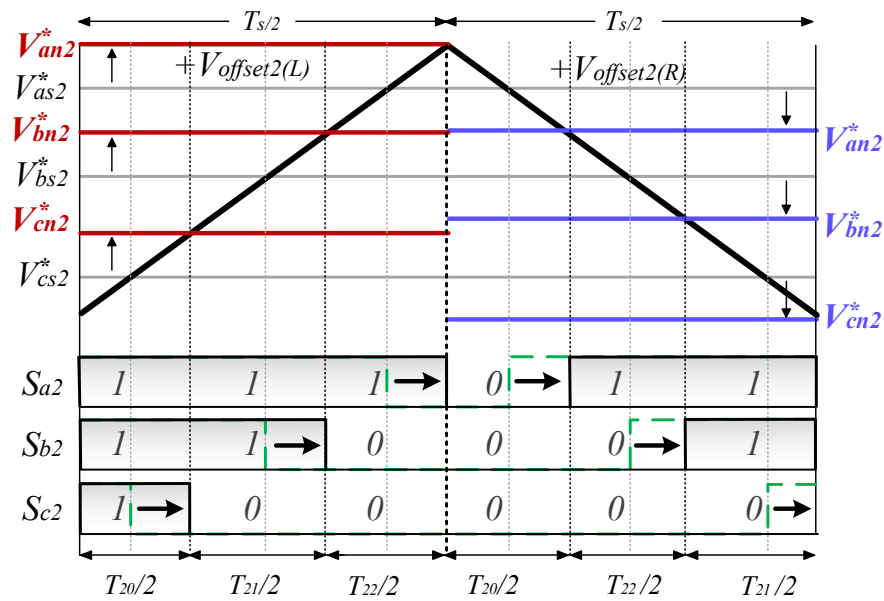


Figure 6. Switching state of inverter 2 with the proposed method.

When the reference pole voltage in inverter 1 is classified into V_{max1}^* , V_{mid1}^* , and V_{min1}^* according to the magnitude, an offset voltage given in Equation (6) is applied during the first half period in order to move the position of the switching state to the left, and an offset voltage of Equation (7) is applied during the remaining half period. The reference pole voltage and switching state of the inverter 1 before and after the offset voltage is applied are shown in Figure 5.

$$V_{offset1(L)} = -V_{min1}^* - V_{dc}/2 \quad (6)$$

$$V_{offset1(R)} = -V_{max1}^* + V_{dc}/2 \quad (7)$$

By applying an offset voltage to the reference pole voltage in inverter 1, the position of the active voltage vector is moved to the start of the switching sequence.

When the reference pole voltage in inverter 2 is classified into V_{max2}^* , V_{mid2}^* , and V_{min2}^* according to the magnitude, an offset voltage of Equation (8) is applied during the first half period in order to move the position of the switching state to the right, and an offset voltage of Equation (9) is applied during the remaining half period. The reference pole voltage and switching state of inverter 2 before and after the offset voltage is applied are shown in Figure 6.

$$V_{offset2(L)} = -V_{max1}^* + V_{dc}/2 \quad (8)$$

$$V_{offset2(R)} = -V_{max1}^* - V_{dc}/2 \quad (9)$$

By applying an offset voltage to the reference pole voltage in inverter 2, the position of the active voltage vector is moved to the end of switching sequence.

3.2. Phase Current Sampling Using PWM Shift Method

If the proposed PWM shift method is used, it is possible to secure four points where the phase current of each motor can be measured through the DC link current sensor during one switching cycle. The phase current measured at the four points synchronized with the active voltage injection time of the dual motors is indicated as Sampling 1~Sampling 4 in order from the left, as shown in Figure 7.

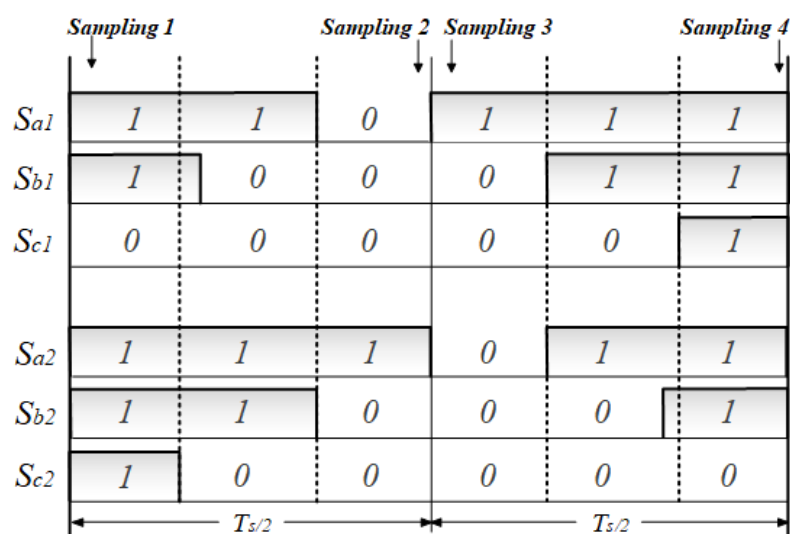


Figure 7. The sampling point according to the proposed method.

Figure 7 shows a switching pattern when the voltage vector of both motors is located in sector 1, using the proposed PWM shift method. The $-i_{c1}$ and i_{a1} of inverter 1 can be measured from sampling 1 and sampling 3, and i_{a2} and $-i_{c2}$ of inverter 2 can be measured from sampling 2 and sampling 4, respectively. The sampling current according to the sector of the voltage vector of each inverter can be represented as shown in Table 2. In other words, the proposed current measurement method can independently obtain the phase current of the dual inverter according to the sector in each voltage vector using the sampled current.

Table 2. Measurable phase currents according to the sector of voltage vector.

Sector	Inverter 1		Inverter 2	
	Sampling 1	Sampling 3	Sampling 2	Sampling 4
1	$-i_{c1}$	i_{a1}	i_{a2}	$-i_{c2}$
2	$-i_{c1}$	i_{b1}	i_{b2}	$-i_{c2}$
3	$-i_{a1}$	i_{b1}	i_{b2}	$-i_{a2}$
4	$-i_{a1}$	i_{c1}	i_{c2}	$-i_{a2}$
5	$-i_{b1}$	i_{c1}	i_{c2}	$-i_{b2}$
6	$-i_{b1}$	i_{a1}	i_{a2}	$-i_{b2}$

3.3. Modifiable Reference Voltage Applied with the Proposed Method

T_{min} is required to sample the DC link current. Each motor needs at least $2T_{min}$ of time during a switching cycle, as only one of the two motors measures current at the time when the active voltage is applied. Therefore, the sum of the applied time of the active voltage vector is less than $T_s - 2T_{min}$.

The magnitude of the reference voltage vectors that can be applied according to these conditions is limited, and the dwell time of the two active voltage vectors of the motor can be obtained by Equations (10) and (11) [7]. The magnitude of the reference voltage satisfying the conditions of the proposed PWM shift method is calculated using Equation (12). The range of the modulation reference voltage presented on the complex plane is shown in Figure 8. Therefore, when applying this algorithm, the range of the modulation reference voltage decreases by the ratio of $2T_{min}/T_s$.

$$T_1 = T_s \frac{3|V^*| \sin(60^\circ - \theta)}{2V_{dc} \sin 60^\circ} \quad (10)$$

$$T_2 = T_s \frac{3|V^*|}{2V_{dc}} \frac{\sin \theta}{\sin 60^\circ} \quad (11)$$

$$V^* \leq \frac{V_{dc}}{\sqrt{3}} T_s \frac{1}{\sin(60^\circ - \theta)} \frac{(T_s - 2T_{min})}{T_s} \quad (12)$$

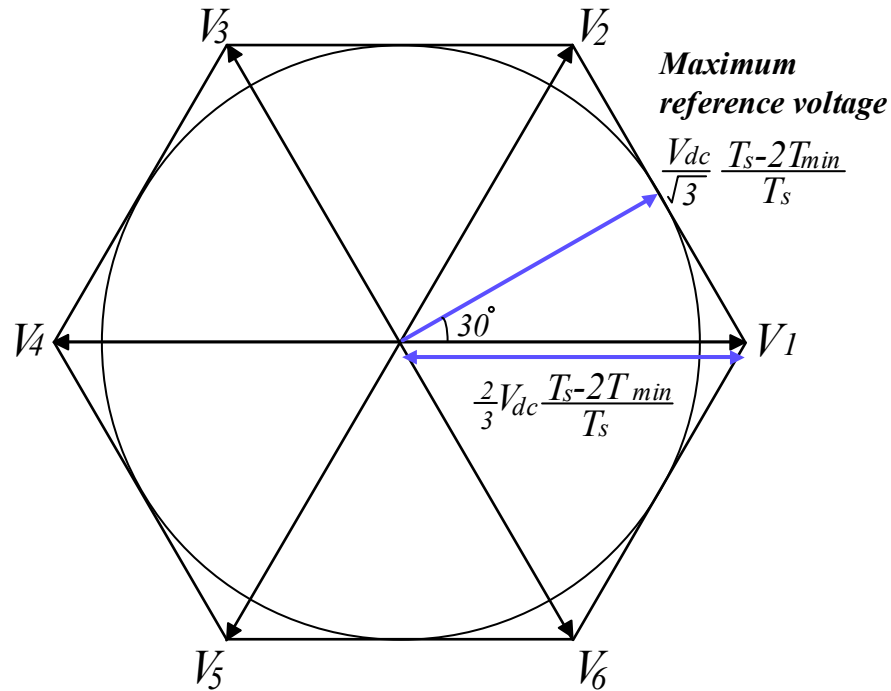


Figure 8. The range of controllable voltage in the proposed method.

4. Proposed Phase Current Reconstruction Method

4.1. The Need for Average Current Estimation

The proposed method for measuring the phase current using a single DC link current sensor is the reconstruction of the phase current using the DC link current that is sequentially measured at the sampling point. The sampled phase current is measured in an inaccurate current containing ripple components as well as an average current component because the sampling time is different. Using the sampled phase current without compensation causes a speed ripple due to a pulsating component in the generated torque, which reduces the overall inverter-motor system performance. Therefore, compensation of the pulsating current by using the mathematical model of the motor was proposed in [16]. However, the sampling point in [22] and the sampling point in the proposed method are different, and hence it is necessary to compensate for the phase current pulsating component according to the proposed method.

4.2. The Need for Average Current Estimation

Figure 9 shows the average current and real phase current when the voltage vector of both motors is located in sector 1. As shown in Figure 9a, the i_{c1} contains a pulsating component ($i_{c1,ripple}$) in the average phase c current in inverter 1 ($i_{c1,avg}$), so the i_{c1} at the sampling point ($i_{c1,sample}$) is different from $i_{c1,avg}$. These differences result in the degradation of inverter-motor system performance. Compensation for the difference between the $i_{c1,avg}$ and $i_{c1,sample}$ is computable using the slope of the phase current according to switching state and dwell time [23]. However, since the phase current sampling point of the proposed method is different from the one in [13], the compensation for the current error is different. Therefore, a compensation method for the pulsating component that is suitable for the proposed sampling time is needed.

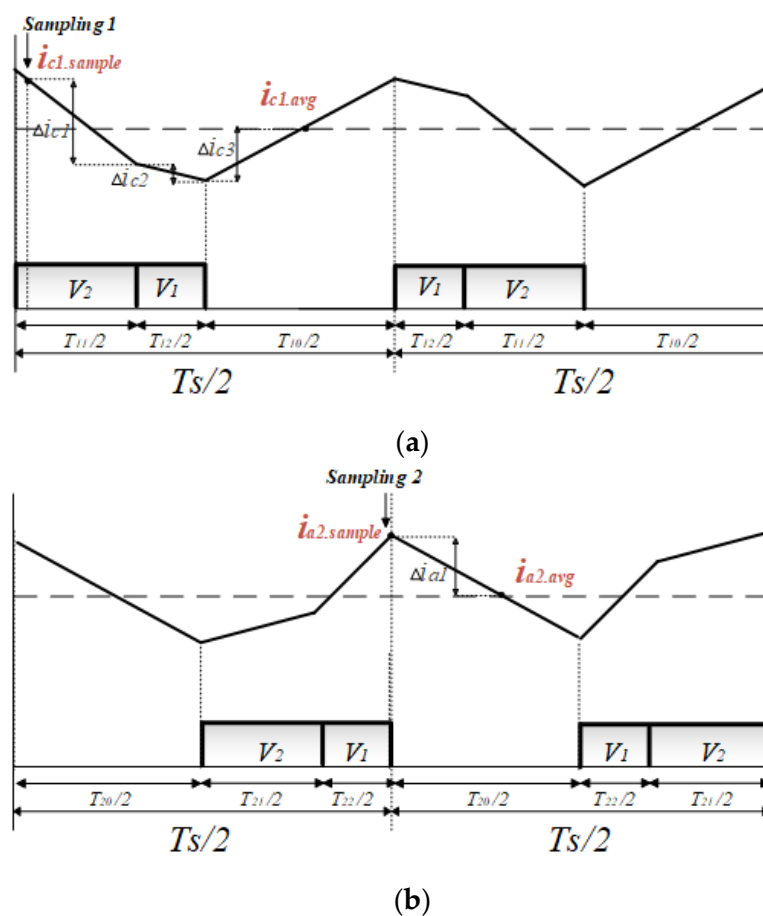


Figure 9. Difference between the proposed sampling and average current: (a) at sampling 1, (b) at sampling 2.

The voltage applied to the resistance of the motor is small, so the resistance component is ignored. The slope of the phase current according to the switching state can be obtained from the equivalent circuit of the three-phase inverter permanent magnet synchronous motor (PMSM) through the Thevenin's equivalent circuit, as shown in Table 3. The back-electromagnetic field (EMF) of PMSM is assumed to be a sinusoidal wave. The dwell time of the active voltage vector can be calculated using the triangle ratio of the reference pole voltage and switching period, as shown in Figure 10.

Table 3. Slope of phase current according to switching state. (adapted from [13].)

Switching State	Slope of Phase a	Slope of Phase b	Slope of Phase c
000	$-\frac{E_a}{L}$	$-\frac{E_b}{L}$	$-\frac{E_c}{L}$
001	$\frac{-3E_a - V_{dc}}{3L}$	$\frac{-3E_b - V_{dc}}{3L}$	$\frac{-3E_c + 2V_{dc}}{3L}$
010	$\frac{-3E_a - V_{dc}}{3L}$	$\frac{-3E_b + 2V_{dc}}{3L}$	$\frac{-3E_c - V_{dc}}{3L}$
011	$\frac{-3E_a - 2V_{dc}}{3L}$	$\frac{-3E_b + V_{dc}}{3L}$	$\frac{-3E_c + V_{dc}}{3L}$
100	$\frac{-3E_a + 2V_{dc}}{3L}$	$\frac{-3E_b - V_{dc}}{3L}$	$\frac{-3E_c - V_{dc}}{3L}$
101	$\frac{-3E_a + V_{dc}}{3L}$	$\frac{-3E_b - 2V_{dc}}{3L}$	$\frac{-3E_c + V_{dc}}{3L}$
110	$\frac{-3E_a + V_{dc}}{3L}$	$\frac{-3E_b + V_{dc}}{3L}$	$\frac{-3E_c - 2V_{dc}}{3L}$
111	$\frac{-E_a}{L}$	$\frac{-E_b}{L}$	$\frac{-E_c}{L}$

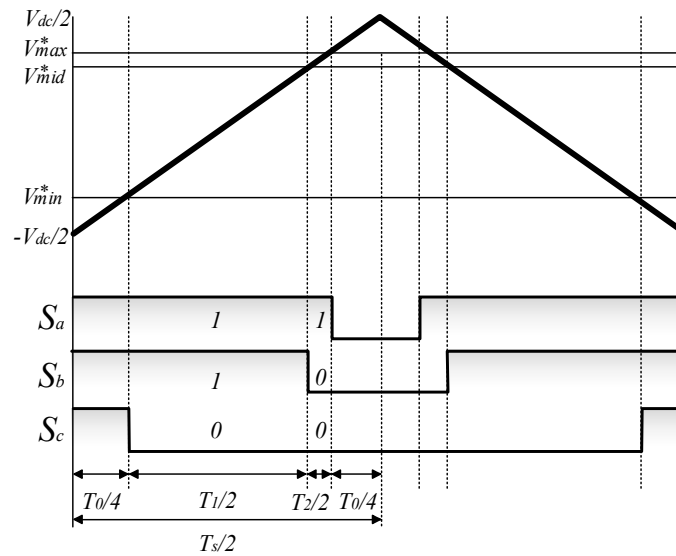


Figure 10. Reference pole voltage and dwell time of switching state.

The dwell time of the active voltage vector and zero voltage vector can be calculated using the reference pole voltage, as shown in Equations (13)–(15) [24].

$$\frac{T_1}{2} = \frac{T_s}{2V_{dc}} (V_{mid}^* - V_{min}^*) \quad (13)$$

$$\frac{T_2}{2} = \frac{T_s}{2V_{dc}} (V_{max}^* - V_{mid}^*) \quad (14)$$

$$\frac{T_0}{4} = \frac{T_s}{4} \left[1 - \frac{1}{V_{dc}} (V_{max}^* - V_{min}^*) \right] \quad (15)$$

4.3. The Need for Average Current Estimation

As shown in Figure 10, the average current can be obtained by calculating four sampling current and error components during a sampling period.

Figure 9a shows the waveform of i_{c1} at sector 1. The $i_{c1,avg}$ can be obtained using $i_{c1,sample}$ and Δi_{c1} , Δi_{c2} , and Δi_{c3} .

$$\Delta i_{c1} = \frac{T_s}{2V_{dc}} (V_{mid1}^* - V_{min1}^*) \frac{V_{dc} - 3E_{c1}}{3L_1} \quad (16)$$

$$\Delta i_{c2} = \frac{T_s}{2V_{dc}} (V_{max1}^* - V_{mid1}^*) \frac{2V_{dc} - 3E_{c1}}{3L_1} \quad (17)$$

$$\Delta i_{c3} = -\frac{T_s}{4} \left[1 - \frac{1}{V_{dc}} (V_{max1}^* - V_{min1}^*) \right] \frac{E_{c1}}{L_1} \quad (18)$$

$$i_{c1,avg} = \frac{T_s}{2L_1} \left[V_{as} - \frac{E_{c1}}{2} \left(1 + \frac{V_{an}^* - V_{cn}^*}{V_{dc}} \right) \right] + i_{c1,samp} \quad (19)$$

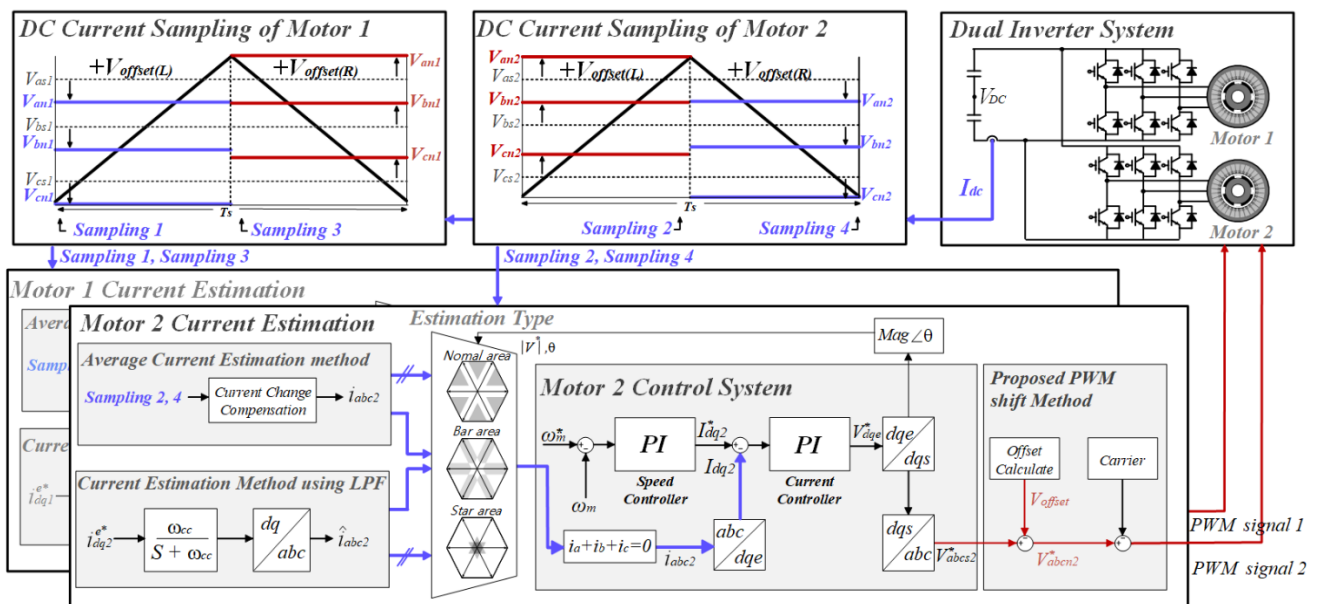
where L_1 is the stator inductance of motor 1, and E_{a1} , E_{b1} , and E_{c1} is back-EMF of phase a , b , and c in motor 1, respectively.

In this way, the average currents can be calculated by the sampling current 2~4 and the compensation value of the current change amount. Furthermore, the equation of compensation can be generalized according to the sector where the reference pole voltage of each motor is located. The equation of average current generalized according to the sector of the sampling current can be summarized as shown in Table 4, where M1 and M2 represent the first and second motor, and max, mid, and min represent the maximum, medium, and minimum value of pole voltage during one period of the switching frequency, respectively.

Table 4. Average current compensation for the proposed sampling currents.

Sampling Current	Generalized Equation of Estimation Average Current
1	$\frac{T_s}{2L_{M1}} \left[V_{max.M1} - \frac{E_{max.M1}}{2} \left(1 + \frac{V_{max.M1}^* - V_{min.M1}^*}{V_{dc}} \right) \right] + i_{max.sample.M1}$
2	$-\frac{E_{min.M2}}{4L_{M2}} \left(1 - \frac{V_{max.M2}^* - V_{min.M2}^*}{V_{dc}} \right) + i_{min.sample.M2}$
3	$\frac{E_{min.M1}}{4L_{M1}} \left(1 - \frac{V_{max.M1}^* - V_{min.M1}^*}{V_{dc}} \right) + i_{min.sample.M1}$
4	$\frac{T_s}{2L_{M2}} \left[V_{max.M2} - \frac{E_{max.M2}}{2} \left(1 + \frac{V_{max.M2}^* - V_{min.M2}^*}{V_{dc}} \right) \right] + i_{max.sample.M2}$

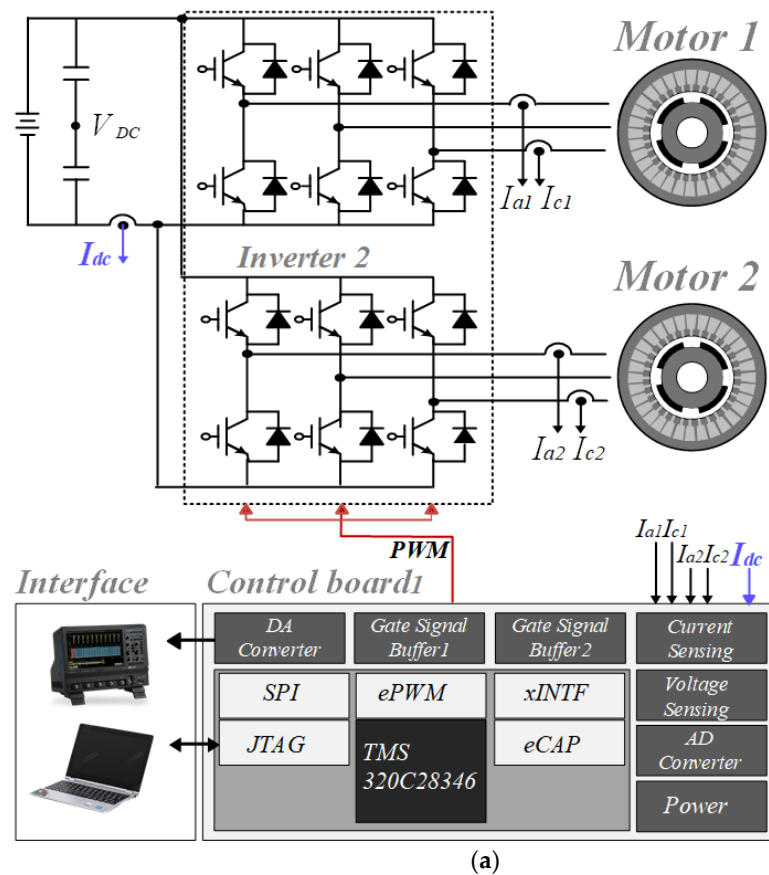
Figure 11 shows the overall control block diagram in a double inverter-motor using a single DC link current sensor. Two phase currents of each inverter-motor system are measured by sampling four times during one switching cycle using the single DC link current sensor. By doing this, the average current is obtained using the proposed average current measurement method when the voltage vector of each inverter is in the measurable area. For the bar region, one phase current of the motor measures using the proposed method, and the other phase current estimates the current using the current estimation method. In the star region, the phase current estimates the current using the current estimation method. This paper estimates the current using the current estimation method in [13], so it can be used in the low modulation region.

**Figure 11.** Block diagram of the overall control system in a dual inverter-motor drive system by using a single DC link current sensor.

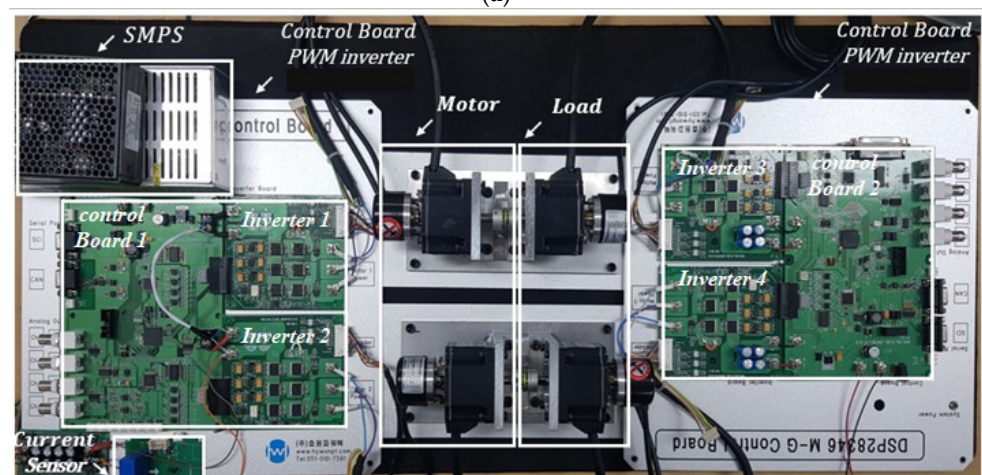
5. Experimental Results

Figure 12a presents the experimental configuration for confirming the effectiveness of the current measurement in a dual inverter-motor drive system using a single DC link current sensor. Figure 12b shows the experimental setup by using two educational M-G sets supported by Hyowon Power Tech. The hardware system consists of two motors, two load units, and two controllers to control them. The main specifications of the inverter-motor are as shown in Table 5. The inverter for motor control consists of six MOSFETs, which use IRFS3107-7P from Infineon. The dead time to prevent a short circuit in the inverter

is set to 1.2 μ s. The two inverters share one DC link capacitor, and a DC link current sensor is installed in order to measure the DC link current. The current sensor used LEM's LA25P. In order to verify the accuracy of the restored current through the proposed current restoration method, two current sensors were additionally installed in each inverter in order to measure the phase current.



(a)



(b)

Figure 12. Configuration of hardware system. (a) System configuration; (b) Experimental M-G set.

Table 5. Parameters of inverter and motor.

Motor		Inverter	
Pole	10	DC link voltage	24 V
Rated power	30 W	Rated current	2.1 A
Stator resistance	1.35 Ω	Turn-on delay	17 ns
Stator inductance	542.5 μ H	Turn-off delay	100 ns
Back-EMF constant	0.0237 V/ w_m	Dead Time	1.2 μ s

The system utilizes the TI's DSP TMS320C28346 microprocessor. The DSP can generate a start of conversion (SOC) signal at a desired time by using an internal ADC with Sallen key filter of 9.8 Hz cut-off frequency; the DC link current is measured at the proposed sampling time. The digital signal from DSP is outputted to DAC8803, using SPI communication, and converted to an analog signal; the experiment was conducted by observing it through an LT264 from Lecroy. The current control cycle of each motor is 100 μ s, and the speed control cycle is set to 1 ms. The sampling frequency is 10 kHz.

Figure 13 shows the waveform of the DC link current measured when the motor is operated at 1000 rpm by using the conventional method [6]. Figure 13a is a waveform of the DC link current during two switching cycles when the conventional method is applied. The DC link current has a region where current can be sampled. Figure 13b shows the i_a and DC link current. The DC link current has a ripple of about 1.5 A.

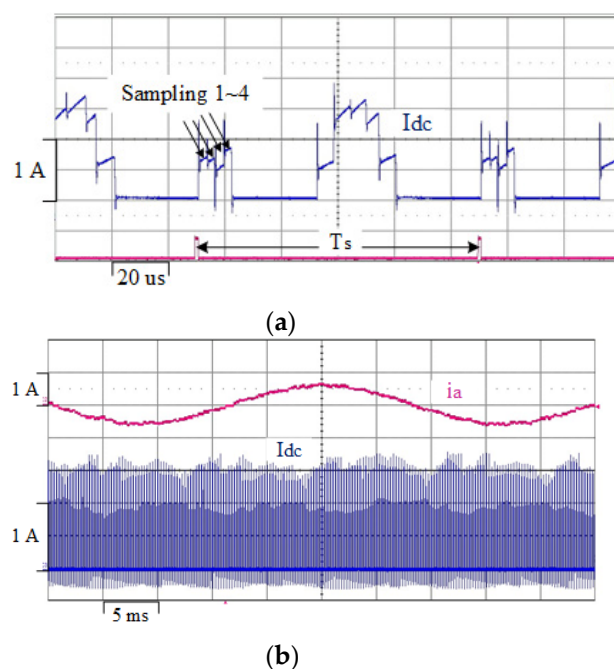


Figure 13. DC link current applied to the conventional method [6] operated at 1000 rpm; (a) two switching cycles; (b) 1.5 cycle fundamental wave.

Figure 14 shows the waveform of the DC link current measured when the motor is operating at 1000 rpm by using the proposed method. Figure 14a is a waveform of the DC link current during two switching cycles when the proposed method is applied. The DC link current has four parts to sample the phase current, and there is no phase current overlap region. The DC link current ripple is reduced compared with the conventional method, as shown in Figure 14b. Therefore, not only the weight of the DC link capacitor but also the loss of the overall inverter-motor system can be reduced.

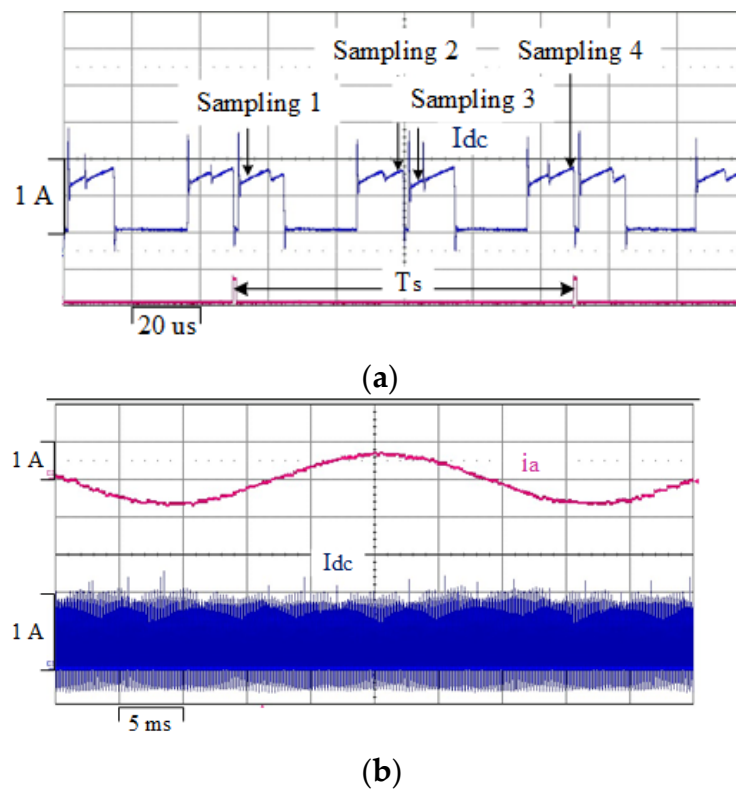


Figure 14. DC link current applied to the proposed method operated at 1000 rpm; (a) two switching cycles; (b) 1.5 cycle fundamental wave.

Figure 15a shows the waveform of i_{a1} measured by phase current sensor (i_{a1_ph}) and current probe (i_{a1_cp}) using the conventional method [6] when the motor is operated at 1500 rpm. Figure 15b shows the results of the fast fourier transform (FFT) in i_{a1_cp} . The i_{a1_cp} in the switching frequency band generates about 35 mA.

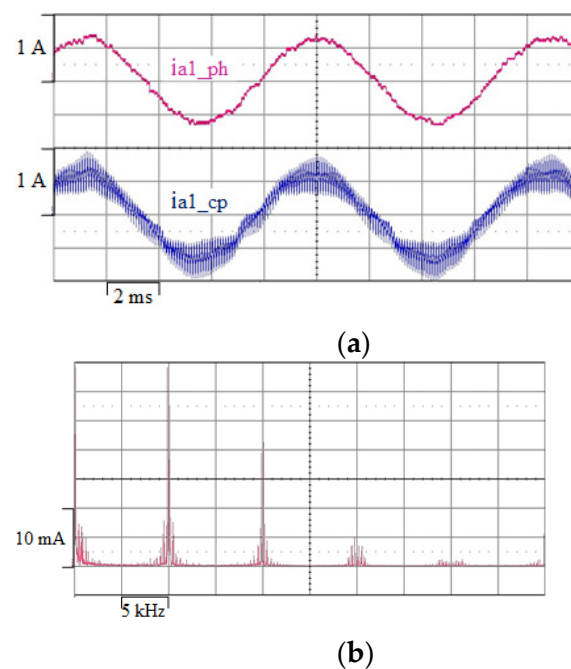


Figure 15. The i_{a1} applied to conventional method [6]; (a) measured results with phase sensor and current probe, (b) FFT results.

Figure 16a shows the waveforms of i_{a1_ph} and i_{a1_cp} using the proposed method when the motor is operated at 1500 rpm. Figure 16b shows the results of the FFT in i_{a1_cp} . The i_{a1_cp} in the switching frequency band generates about 5 mA. The proposed method uses a symmetric active voltage vector, thus the harmonics in the switching frequency band is reduced by about 85%.

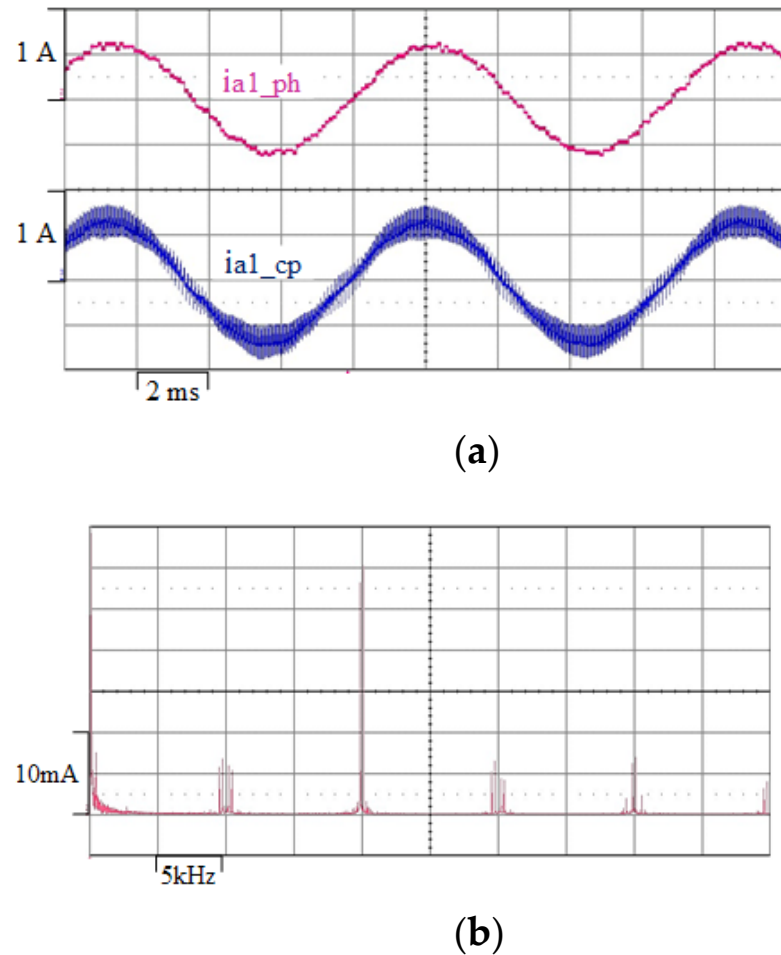
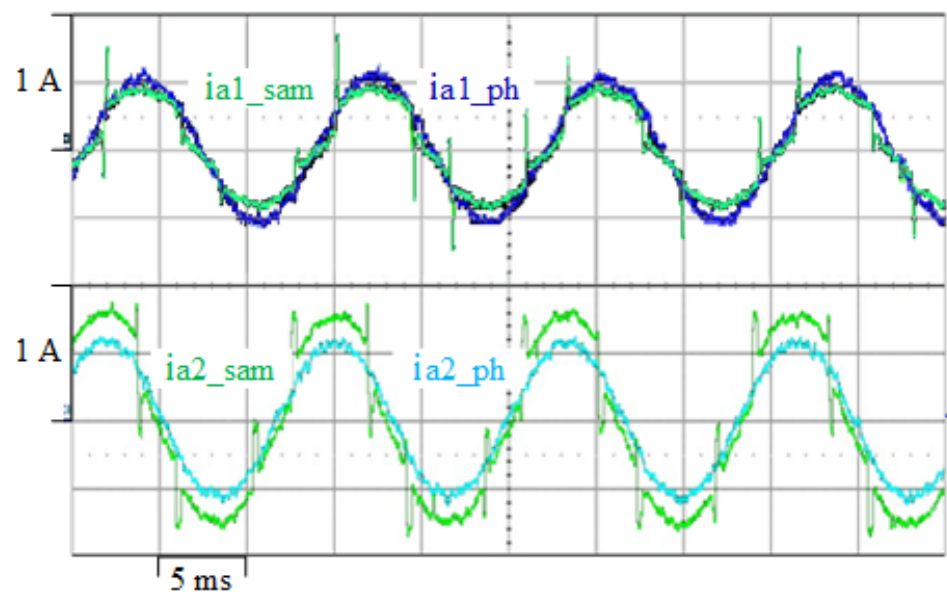
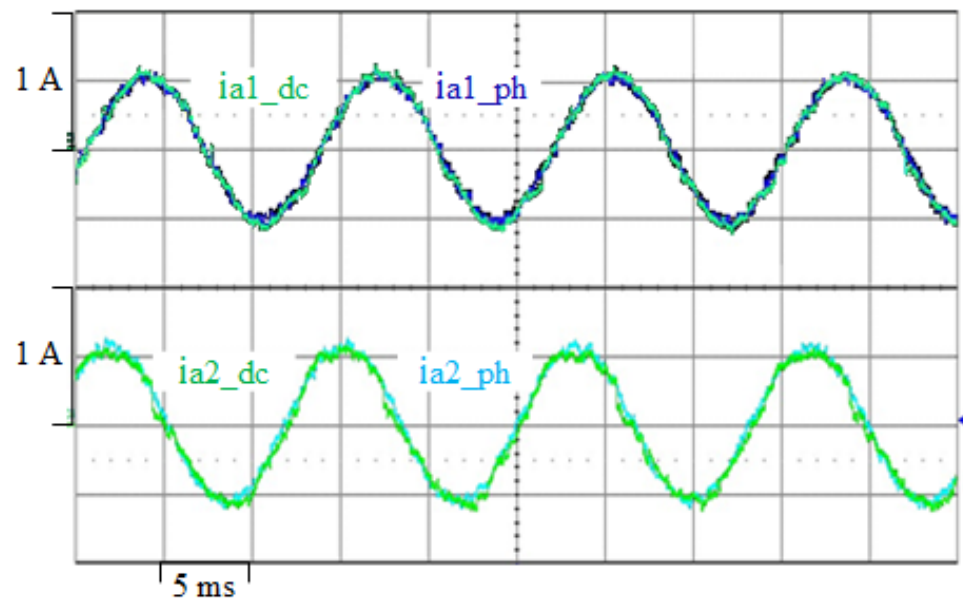


Figure 16. The i_{a1} applied to the proposed method: (a) measured results with phase sensor and current probe; (b) FFT results.

Figure 17a shows the waveforms of the phase currents of inverter 1 and inverter 2 obtained from sampling the DC link current and the current measured by phase current sensors. i_{a1_sam} and i_{a2_sam} represent the phase current obtained from sampling the DC link current for inverter 1 and inverter 2, respectively. i_{a1_ph} and i_{a2_ph} are the currents measured using the phase current sensors of inverter 1 and inverter 2, respectively. The i_{a1_sam} and i_{a2_sam} have a large pulsating component in the measurable region, and cannot be measured in the unmeasurable region. In the measurable region, the phase current reconstruction is done by using average current compensation. In the unmeasurable region, the phase current is estimated by using the reference current. The i_{a1_dc} and i_{a2_dc} can be obtained by using i_{a1_sam} and i_{a2_sam} and the compensation method, as shown in Figure 17b. The current restored by the DC link current sensor and the current measured by using the phase current sensor are almost identical. Therefore, the adequacy of the steady state was confirmed in the same control state of the proposed algorithm.



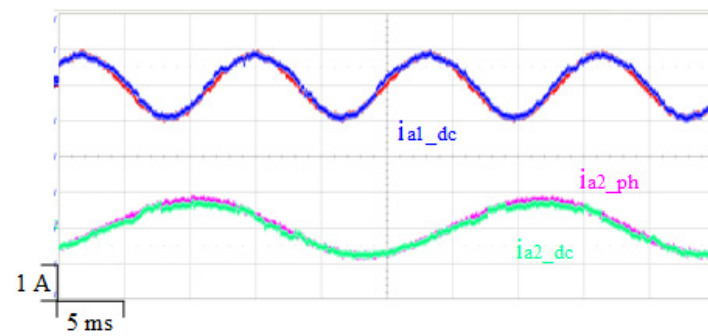
(a)



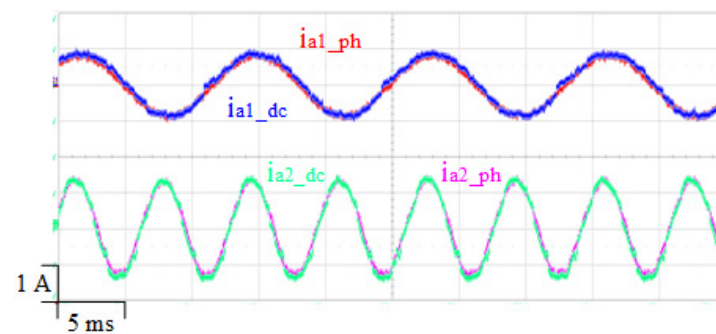
(b)

Figure 17. Phase current of two motors according to measurement methods operated at 1000 rpm. (a) The sampling current measured by a DC link current sensor and the current measured by a phase current sensor; (b) The restored current and the current measured by a phase current sensor.

When the motor is controlled under different conditions, the speed of motor 1 was fixed and motor 2 was changed to confirm the adequacy of the proposed algorithm. Figure 18a shows a phase current measured by different methods when controlling motor 1 to a speed of 1000 rpm and motor 2 to a speed of 500 rpm. Figure 18b shows the phase current measured by different methods when controlling motor 1 to a speed of 1000 rpm and motor 2 to a speed of 2000 rpm. As shown in Figure 18, when the speed of the dual motor is different, the restored current measured by a DC link current sensor can be measured independently and accurately.



(a)



(b)

Figure 18. Measured phase currents of two motors according to motor 1 operated at 1000 rpm and motor 2 operated at either (a) 500 rpm or (b) 2000 rpm.

In Figure 19, in order to verify the transient characteristics of the proposed algorithm, motor 1 was fixed and the speed of motor 2 was increased from 1000 rpm to 2000 rpm. It was confirmed that i_{a2_ph} and i_{a2_dc} were similar. When the speed reference is changed in motor 2, i_{qe2} generates a flow of 2.1 A. It is possible to measure the current using the DC link current sensor in the transient response.

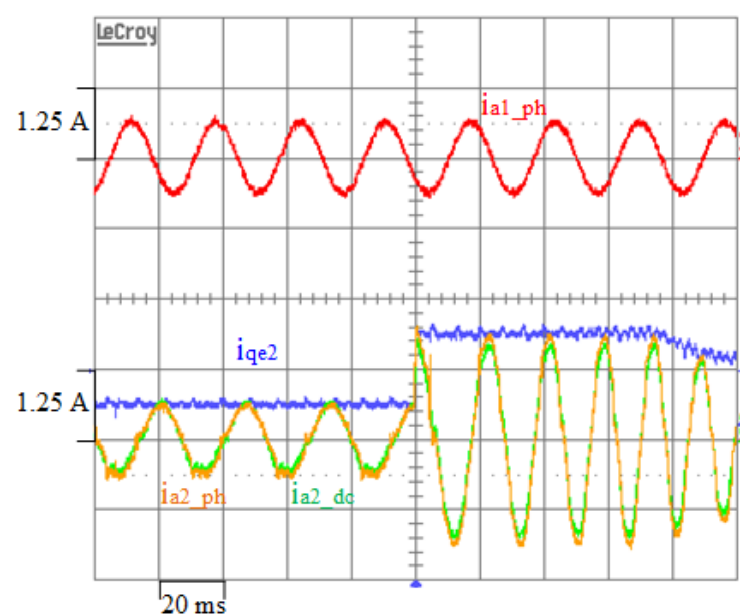


Figure 19. The current of two motors in the transient state.

6. Conclusions

In this paper, a current reconstruction method using a single DC link current sensor in a dual inverter-motor system was proposed. The measurable area is considered as follows. First, a PWM shift method was proposed that can secure phase current measurement time while minimizing phase current ripple. Second, a sampling point for the phase current measurement was proposed. Finally, an average current calculation method was proposed in order to compensate for the pulsation component included in the proposed sampling current. In this method, the sampling points to measure the phase current were secured by moving the switching pattern of two motor in opposite directions. In order to apply this to three or more motors, a zero voltage vector must be applied to two motors and an active voltage vector must be applied to one motor, so a new algorithm is needed. In considering the unmeasurable area, the current is estimated using [13]. Therefore, it can be used in the low modulation region. Compared with the conventional method, the phase current ripple is reduced in the switching frequency band by about 85%. At less than 50% load, DC current ripple is reduced compared to the conventional method. Furthermore, the current can be independently restored at various speeds and load conditions from the single DC link current sensor.

Author Contributions: Conceptualization, J.-H.J. and J.-M.K.; methodology, S.-I.H. and S.-H.C.; software, S.-H.C.; validation, J.-H.J. and J.-M.K.; formal analysis, S.-H.C. and J.-M.K.; investigation, S.-I.H. and S.-H.C.; data curation, S.-I.H. and S.-H.C.; writing—original draft preparation, S.-I.H.; writing—review and editing, J.-H.J. and J.-M.K.; visualization, S.-I.H. and S.-H.C.; supervision, J.-H.J. and J.-M.K. All authors have read and agreed to the published version of the manuscript.

Funding: This work was supported by BK21FOUR, Creative Human Resource Education and Research Programs for ICT Convergence in the 4th Industrial Revolution.

Institutional Review Board Statement: Not applicable.

Informed Consent Statement: Not applicable.

Data Availability Statement: Accepted and complied with.

Conflicts of Interest: The authors declare no conflict of interest.

References

- Kim, H.D.; Perry, A.T.; Ansell, P.J. A review of Distributed Electric Propulsion Concepts for Air Vehicle Technology. In Proceedings of the 2018 AIAA/IEEE EATS, Cincinnati, OH, USA, 12–14 July 2018.
- Shamiyeh, M.; Rothfeld, R.; Hornung, M.A. Performance Benchmark of Recent Personal Air Vehicle Concepts for Urban Air Mobility. In Proceedings of the 31th Congress of the International Council of the Aeronautical Sciences, Belo Horizonte, Brazil, 9–14 September 2018.
- Song, W.; Pei, X.; Xi, J.; Zeng, X. A Novel Helical Superconducting Fault Current Limiter for Electric Propulsion Aircraft. *IEEE Trans. Transp. Electr.* **2021**, *7*, 276–286. [\[CrossRef\]](#)
- Sarlioglu, B.; Morris, C.T. More Electric Aircraft: Review, Challenges, and Opportunities for Commercial Transport Aircraft. *IEEE Trans. Transp. Electr.* **2015**, *1*, 54–64. [\[CrossRef\]](#)
- Rosero, J.A.; Ortega, J.A.; Aldabas, E.; Romeral, L.A. Moving Towards a More Electric Aircraft. *IEEE Aerosp. Electron. Syst. Mag.* **2007**, *22*, 3–9. [\[CrossRef\]](#)
- Ye, H.; Emadi, A. A Six-Phase Current Reconstruction Scheme for Dual Traction Inverters in Hybrid Electric Vehicles with a Single DC-Link Current Sensor. *IEEE Trans. Veh. Technol.* **2014**, *63*, 3085–3093. [\[CrossRef\]](#)
- Van Der Broeck, H.W.; Skudelny, H.C.; Stanke, G.V. Analysis and Realization of a Pulsewidth Modulator Based on Voltage Space Vectors. *IEEE Trans. Ind. Appl.* **1988**, *24*, 142–150. [\[CrossRef\]](#)
- Gan, C.; Wu, J.; Wang, N.; Hu, Y.; Cao, W.; Yang, S. Independent Current Control of Dual Parallel SRM Drive Using a Public Current Sensor. *IEEE/ASME Trans. Mechatron.* **2017**, *1*, 392–401. [\[CrossRef\]](#)
- Schiedermeier, M.; Rettner, C.; Heilmann, M.; Schneider, F.; Marz, M. Interference of automotive HV-DC-systems by traction voltage-source-inverters (VSI). In Proceedings of the 2019 IEEE Transportation Electrification Conference, Bengaluru, India, 17–19 December 2019.
- Liu, T.; Fadel, M. An Efficiency-Optimal Control Method for Mono-Inverter Dual-PMSM Systems. *IEEE Trans. Ind. Appl.* **2018**, *2*, 1737–1745. [\[CrossRef\]](#)
- Wang, X.; Wang, Z.; Xu, Z.; He, J.; Zhao, W. Diagnosis and Tolerance of Common Electrical Faults in T-Type Three-Level Inverters Fed Dual Three-Phase PMSM Drives. *IEEE Trans. Power Electron.* **2020**, *2*, 1753–1769. [\[CrossRef\]](#)

12. Ha, J.I. Voltage Injection Method for Three-Phase Current Reconstruction in PWM Inverters Using a Single Sensor. *IEEE Trans. Power Electron.* **2009**, *24*, 767–775.
13. Park, C.-H.; Kim, D.-Y.; Yeom, H.-B.; Son, Y.-D.; Kim, J.-M. A Current Reconstruction Strategy Following the Operation Area in a 1-Shunt Inverter System. *Energies* **2019**, *12*, 1423. [\[CrossRef\]](#)
14. Wang, W.; Yan, H.; Xu, Y.; Zou, J.; Zhang, X.; Zhao, W.; Buticchi, G.; Gerada, C. New Three-Phase Current Reconstruction for PMSM Drive With Hybrid Space Vector Pulsewidth Modulation Technique. *IEEE Trans. Power Electron.* **2021**, *1*, 662–673. [\[CrossRef\]](#)
15. Lee, W.-C.; Hyun, D.-S.; Lee, T.-K. A Novel Control Method for Three-Phase PWM Rectifiers Using a Single Current Sensor. *IEEE Trans. Power Electron.* **2000**, *15*, 861–870.
16. Lu, H.; Cheng, X.; Qu, W.; Sheng, S.; Li, Y.; Wang, Z. A Three-Phase Current Reconstruction Technique Using Single DC Current Sensor Based on TSPWM. *IEEE Trans. Power Electron.* **2014**, *3*, 1542–1550.
17. Lin, Y.-K.; Lai, Y.-S. PWM Technique to Extend Current Reconstruction Range and Reduce Common-Mode Voltage for Three-Phase Inverter using DC-link Current Sensor Only. In Proceedings of the 2011 IEEE ECCE, Phoenix, AZ, USA, 17–22 September 2011.
18. Lai, Y.-S.; Lin, Y.-K.; Chen, C.-W. New Hybrid Pulsewidth Modulation Technique to Reduce Current Distortion and Extend Current Reconstruction Range for a Three-Phase Inverter Using Only DC-link Sensor. *IEEE Trans. Power Electron.* **2013**, *28*, 1331–1337. [\[CrossRef\]](#)
19. Saritha, B.; Janakiraman, P.A. Sinusoidal Three-Phase Current Reconstruction and Control Using a DC-Link Current Sensor and a Curve-Fitting Observer. *IEEE Trans. Ind. Electron.* **2007**, *54*, 2657–2664. [\[CrossRef\]](#)
20. Kim, K.-S.; Yeom, H.-B.; Ku, H.-K.; Kim, J.-M.; Im, W.-S. Current Reconstruction Method with Single DC-Link sensor based on the PWM inverter and AC motor. In Proceedings of the IEEE ECCE, Pittsburgh, PA, USA, 14–18 November 2014.
21. Kim, H.-J.; Kim, J.-M.; Kim, J.-M. Current measurement and control method of HVAC integration system through DC link single current sensor. *J. Power Electron.* **2020**, *20*, 1243–1249. [\[CrossRef\]](#)
22. Bing, Z.; Du, X.; Sun, J. Control of Three-Phase PWM Rectifiers Using a Single DC Current Sensor. *IEEE Trans. Power Electron.* **2010**, *26*, 1800–1808. [\[CrossRef\]](#)
23. Green, T.C.; Williams, B.W. Derivation of motor line-current waveforms from the DC-link current of an inverter. *IEE Proc.* **1989**, *136*, 196–204. [\[CrossRef\]](#)
24. Chung, D.-W.; Kim, J.-S.; Sul, S.-K. Unified voltage modulation technique for real-time three-phase power conversion. *IEEE Trans. Ind. Appl.* **1998**, *34*, 374–380. [\[CrossRef\]](#)